ACS Combinatorial Science

Research Article

pubs.acs.org/acscombsci

NGR Peptide Ligands for Targeting CD13/APN Identified through Peptide Array Screening Resemble Fibronectin Sequences

Rania Soudy, Sahar Ahmed, and Kamaljit Kaur*

Faculty of Pharmacy and Pharmaceutical Sciences, University of Alberta, Edmonton, Alberta, Canada, T6G 2E1

Supporting Information

ABSTRACT: Peptides containing the Asn-Gly-Arg (NGR) motif are known to bind CD13 isoforms expressed in tumor vessels and have been widely used for tumor targeting. Residues flanking the NGR sequence play an important role in modulating the binding affinity and specificity of NGR for the CD13 receptor. Herein, we have used a rapid, easy, and reliable peptide array−whole cell binding assay for screening a library of NGR peptides with different flanking residues. A peptide array consisting of forty-five NGR containing peptides was synthesized on a cellulose membrane, followed by screening against CD13 positive (HUVEC and HT-1080) and CD13 negative cell lines (MDA-MB-435 and MDA-MB-231). The library screening led to the identification of five cyclic and acyclic NGR peptides that display higher binding (up to 5-fold) to CD13 positive cells with negligible binding to CD13 negative cell lines when compared to the lead sequence cyclic CVLNGRMEC. Peptides with high binding affinity for the CD13 positive cells also showed improved in vitro cellular uptake and specificity using flow cytometry and fluorescence microscopy. Interestingly, the identified peptides resemble the NGR sequences present in the human fibronectin protein. These NGR peptides are promising new ligands for developing tumor vasculature targeted drugs, delivery systems and imaging agents with reduced systemic toxicity.

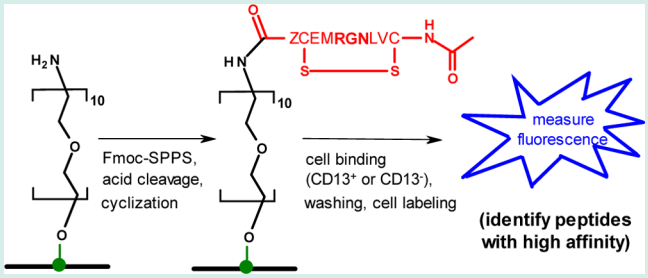

KEYWORDS: *peptide array-cell binding, aminopeptidase N/CD13, NGR sequence, tumor targeting*

INTRODUCTION

Targeted drug therapy to tumor vasculature has emerged as one of the most promising approaches for the treatment of cancer. In this approach, specific targeting moieties, such as peptides or antibodies, actively guide drugs to receptors that are uniquely expressed on tumor vascular tissue.[1,2] Some of these unique molecular markers expressed within tumor associated vessels include $\alpha v\beta 3$ and $\alpha v\beta 5$ integrins,[3,4] aminopeptidase N (APN or CD13),[5] vascular endothelial growth factor receptors (VEGFRs),[6,7] and matrix metalloproteinases (MMPs).[8] The differential expression of these cancer cell biomarkers make them attractive targets for selective delivery of chemotherapeutic drugs and diagnostic moieties.[9,10]

APN (CD13) is a Zn^{2+} dependent metalloprotease that has been implicated in various cell functions, such as proliferation, invasion, and angiogenesis.[11,12] Specific APN isoforms are highly expressed in various tumors and angiogenic cells, and these are different from the APN forms expressed by the endothelium of normal blood vessels.[13] Recently it has been shown that APN is selectively expressed in vascular endothelial cells, such as human umbilical vein endothelial cells (HUVEC), and plays multiple roles in angiogenesis.[12,14] Thus CD13 has become an attractive molecular tumor marker and potential therapeutic target.[5,15] In vivo screening of phage libraries led to the discovery of the Asn-Gly-Arg (NGR) peptide motif that binds primarily to the CD13 receptor expressed in the endothelium of angiogenic blood vessels.[16,17] The selective tumor homing ability of NGR led to the use of this peptide for targeted delivery of various antitumor compounds, such as chemotherapeutic drugs,[17] cytokines,[18] viral particles,[19] and liposomes[20] specifically to tumor vessels. Notably, the NGR sequence is also present in fibronectin (FN), an extracellular matrix protein involved in several key cellular processes.[21] Human FN is a large glycoprotein that contains primarily three types of repeating modules, type I, II, and III. NGR with different flanking residues is present in each of the repeating modules of human FN.

Phage display technology has been employed for selecting peptides with high affinity for CD13 associated with the angiogenic blood vessels. Several NGR containing peptide sequences have been identified, such as disulfide bond cyclized CNGRC (cCNGRC) and cCVLNGRMEC, as well as linear analogues GNGRG and NGRAHA.[17,22] The peptide sequence cCNGRC has been coupled to different anticancer compounds, such as doxorubicin,[17,23] cisplatin,[24] proapototic peptides,[25] and tumor necrosis factor-α (TNF).[18] NGR conjugated to TNF (NGR-hTNF) is in phase II clinical trials.[26,27] In addition to disulfide cyclized sequences, an N- to C-terminal amide bond cyclized cKNGRE sequence has been studied that displayed enhanced binding affinity for tumor targeting applications.[28]

Received: May 28, 2012
Revised: September 26, 2012
Published: October 2, 2012

Pentapeptide analogues of NGR synthesized via on-resin click chemistry have also been developed and show specific binding to purified CD13 receptor, as well as to cell lysates from $CD13^+$ SKOV-3 cancer cells.[29] Structure−function studies with different NGR peptide sequences suggest that the molecular scaffold in which NGR residues are embedded could affect binding affinity, specificity, and peptide stability. For instance, studies with cyclic CNGRC and linear GNGRG peptides showed that the presence of disulfide constraint enhances interaction with CD13, improving targeting ability 10-fold.[30] Modification of cCNGRC with proline to produce cCPNGRC improved overall binding affinity to APN and led to 30-fold lower IC_{50} for the inhibition of APN proteolytic activity.[31] In addition, it has been shown that flanking residues play an important role in NGR to isoaspartate-glycine-arginine (isoDGR) conversion with concomitant exchange of receptor affinity from CD13 to $\alpha v\beta 3$ integrin.[32]

The above studies demonstrate that the specificity and affinity of NGR peptides for the CD13 receptor can be improved by altering the NGR flanking residues. To further explore this hypothesis, we designed and screened a library of NGR sequences based on the lead cCVLNGRMEC peptide to identify new peptides with enhanced binding affinity for CD13. A library of 45 peptides was synthesized in an array format on cellulose membrane and the library was screened against CD13-positive and CD13-negative cell lines using a peptide array-whole cell binding assay. We have previously shown that peptide array-whole cell binding is a complementary method to phage display for the identification of peptides with higher binding affinity and specificity for cancer cells.[33] Here we show that the library screening led to the identification of five NGR peptides (peptides **5**, **14**, **21**, **22**, and **34**) that display higher binding (up to 5-fold) to $CD13^+$ cells with negligible binding to $CD13^-$ cell lines when compared to the lead sequence. These peptides with augmented affinity for the $CD13^+$ cells also show improved in vitro cellular uptake and specificity using soluble FITC-labeled peptides. Interestingly, the peptides identified here are similar to or resemble the NGR sequences present in the human FN protein.

RESULTS AND DISCUSSION

Integrin $\alpha v\beta 3$ and CD13 (APN) are the most studied receptors for targeting endothelial cells involved in tumor angiogenesis.[3,5,34] The structure of RGD peptides has been optimized and several RGD peptides targeting integrins are undergoing preclinical evaluation for tumor targeting.[35,36] While equally promising for targeting the CD13 receptor, the NGR sequence has been less explored. In order to optimize the binding affinity and specificity of peptides containing the NGR sequence, we designed a peptide array to screen against CD13 expressing cell lines ($CD13^+$), and cells that do not express CD13 ($CD13^-$).

Engineering NGR-Based Peptide Library. Forty-five NGR peptide sequences, cyclic and acyclic, based on the CVLNGRMEC sequence[16] (peptide **1**, Table 1) were synthesized. The key NGR motif was maintained in all the peptides, except the negative controls. Peptide **1**, the lead 9-mer peptide, containing the NGR motif was originally identified by phage display that specifically targets tumor blood vessels.[17] Later it was found that the NGR motif targets the CD13 in the angiogenic vasculature and in many tumor cell lines.[22] Peptides **2**−**7** are previously reported sequences or derivatives of reported sequences.[17,21,37,38] Met was replaced with Nle in peptide **2** as well as in the designed sequences to eliminate problems associated with Met oxidation. NGR containing peptide **3** was isolated by in vivo phage display to target $\alpha_5\beta_1$ integrins.[37] Peptides **4** and **5** are conserved NGR sequences present in the natural protein, fibronectin.[22] Peptide **6** is a

Table 1. Sequence of the NGR Peptide Library and the Relative Cell Adhesion Capacity of the Peptides[a]

			relative cell adhesion	
	peptide	peptide sequence	HUVEC	HT-1080
	1	CVLNGRMEC	1.0	1.0
	2	CVLNGR**X**EC	1.7	1.6
	3	NGRAHA	2.6	1.6
	4	LNGRE	3.2	3.3
	5	YNGRT	5.4	5.5
	6	LNGRAHA	0.4	0.5
	7	cNGRGEQc	1.9	1.3
group 1	**8**	C**A**LNGRXEC	1.3	2.7
	9	CV**A**NGRXEC	3.1	1.6
	10	CVLNGR**A**EC	1.2	2.4
	11	CVLNGRX**A**C	1.1	0.6
	12	CVLNGRXE**A**	2.4	2.1
group 2	**13**	CVLNGRXC	1.2	2.7
	14	CVLNGREC	3.4	3.9
	15	CVLNGRC	1.9	2.7
	16	CLNGRXEC	0.4	0.8
	17	CVNGRXEC	1.1	2.6
	18	CNGRXEC	0.7	1.1
	19	CLNGRXC	0.5	0.9
	20	CVNGREC	0.8	2.2
	21	CNGRC	3.5	4.2
	22	KCNGRC	4.3	4.8
	23	**K**VLNGRXE	2.0	3.1
	24	**G**VLNGRME**G**	1.2	0.8
	25	**G**VLNGRXE**G**	1.2	1.6
	26	**G**NGR**G**	2.7	2.8
group 3	**27**	C**I**LNGRXEC	1.2	1.3
	28	C**T**LNGRXEC	0.5	1.3
	29	C**Z**LNGRXEC	0.3	1.7
	30	CV**V**NGRXEC	2.1	2.7
	31	CV**Z**NGRXEC	1.5	2.1
	32	CV**X**NGRXEC	3.1	3.9
	33	CV**S**NGRXEC	2.1	3.9
	34	CVLNGR**S**EC	3.2	4.5
	35	CVLNGRX**D**C	3.1	3.7
	36	CVLNGRX**K**C	1.7	2.0
	37	**c**VLNGRXE**c**	1.1	3.1
negative control	**38**	CKLARAXEC	0.7	0.9
	39	VLARAXE	1.0	0.6
	40	CVL**Q**GRXEC	0.4	2.2
	41	CVLARAXEC	0.9	2.1
	42	AVLXGXEA	2.3	5.4
	43	VLGXE	0.4	0.6
	44	CVLGXEC	1.2	2.5
	45	CARAC	0.6	0.8

[a]aa substitution is underlined; X = norleucine; Z = β-alanine, lower case letter = D-aa. RCA is the average ratio of fluorescence of a peptide (due to bound cells) divided by that of peptide **1**.

dx.doi.org/10.1021/co300055s | ACS Comb. Sci. 2012, 14, 590−599

hybrid of peptides **3** and **4**. Peptide **7** was identified by Lau and co-workers as a peptide ligand for adhesion and proliferation of human lung cancer cells.[38]

The remaining peptides in the array were separated into three groups, as shown in Table 1. Peptides **8**−**12** (group 1) consisted of an alanine scan, replacing each residue in peptide **2** with Ala, except the NGR sequence. Next, sequences with N- or C-terminal residues deleted yielded shorter cyclic peptides **13**−**22** ranging from 5-mer to 8-mer. Peptides **23**−**26** were linear derivatives of peptide **2**, designed to study the effect of the disulfide constraint on targeting efficiency. In addition, the linear NGR motif, GNGRG (**26**), is present in the wild type fibronectin sequence.[21,22]

Peptides **27**−**37** (group 3) involved conservative substitution of N- (Val2 or Leu3) or C-terminal (Nle7 or Glu8) residues in peptide **2** with different amino acids. For instance, Val2 was substituted with either nonpolar Ile or β-Ala to give peptides **27** and **29**, respectively, or with polar Thr to give peptide **28**. Likewise, Leu3 was substituted with nonpolar Val, β-Ala or Nle in analogues **30**−**32**, respectively. Peptides **33** and **34** have a hydroxyl-containing amino acid (Ser) next to Asn or Arg residues, respectively, of the NGR motif. The C-terminal Glu8 was similarly replaced to give peptides with either negatively charged Asp in analogue **35**, or positively charged Lys in analogue **36.** Peptide **37** has two L-cysteines replaced with D-cysteines. Lastly, peptides **38**−**45** were designed as negative controls with scrambled sequences and varying length, and were devoid of the NGR motif.

The peptide library, with each entry in duplicate (Table 1), was synthesized on noncleavable cellulose membrane (amino-PEG500) using SPOT synthesis, where the C-terminus of the peptide was attached to the surface of the amino-PEG500 cellulose membrane through β-ala spacer as described previously.[33] Each residue was added to the free amino functional group using a stepwise Fmoc-SPPS procedure. Each peptide was synthesized at a concentration of approximately 50 nmoles spread on the membrane in a spot with a diameter of 4 mm. After complete synthesis of the array, the peptides were oxidized (cyclized) on the membrane by incubation in 20% aqueous DMSO at 4 °C for 24 h followed by overnight incubation at room temperature. The stepwise incubations were done to decrease the possibility of degradation and transition of NGR to *iso*DGR/DGR, which is accompanied by the loss of CD13 binding. Recent studies have shown that compounds containing the NGR motif can rapidly deamidate and generate isoDGR spontaneously at elevated pH and temperature.[39]

Level of Aminopeptidase N (or CD13) Expression. Four cells lines [HUVEC human umbilical cord, HT-1080 fibrosarcoma, MDA-MB-435 melanoma and MDA-MB-231 breast cancer cells] were evaluated for APN/CD13 expression using flow cytometry. The CD13 expression level was quantified by the mean fluorescence of the cells after incubation with FITC-labeled antihuman CD13 antibody (CD13 mAb or WM15). The results showed that HUVEC and HT-1080 cells expressed high level of CD13 with mean cell fluorescence 90 and 46.7, respectively, whereas, MDA-MB-231 and MDA-MB-435 did not express this receptor and show mean cell fluorescence of 7 and 5.2, respectively (Figure 1). These results matched with the reported CD13 expression levels of different cell lines.[40] For subsequent experiments, HUVEC and HT-1080 were selected as $CD13^+$, while MDA-MB-435 and MDA-MB-231 served as $CD13^-$ or negative control cell lines.

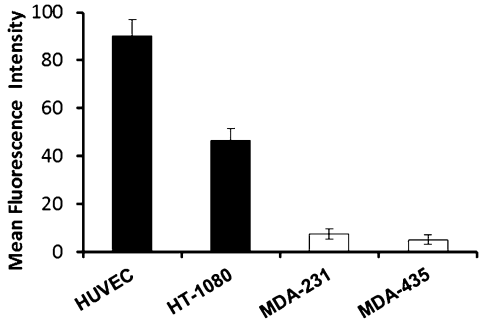

Figure 1. Expression of aminopeptidase N (APN or CD13) in the cell lines used in this study. Four cell lines, $CD13^+$ (HUVEC and HT-1080) and $CD13^-$ (MDA-435 and MDA-231), were incubated with FITC-labeled monoclonal antihuman CD13 antibody (WM15) for 30 min at 4 °C. After washing the cells, the fluorescence of the bound antibody was analyzed by flow cytometry. The mean fluorescence intensity of the cells is shown.

Peptide Array-Cell Binding Assay. We have previously shown that peptide arrays on cellulose membranes are excellent platforms for whole cell binding and screening of peptides with high relative affinity for the intact cells.[33] Here the NGR peptide array was incubated with each of the above four cell lines to screen for $CD13^+$ cell binding peptides, and the experiment was repeated once. No blocking of the membrane was done before adding the cells, and after each experiment the cellulose membrane was regenerated to be reused. After incubation, the cells that bound to the cellulose membrane were labeled with CyQuant dye followed by detection with fluorescence. The array was visualized using Kodak imager with excitation at 485 nm and emission at 530 nm. The fluorescence intensity of the spots (shown in Figure 2) reflecting the amount of bound cells was measured. All the peptides were compared to the wild type peptide **1** and the relative cell adhesion ratio for each peptide binding to cells was determined. The relative cell adhesion ratio for the $CD13^+$ cells, HUVEC and HT-1080, is listed in Table 1.

In general, $CD13^+$ cell lines (HUVEC and HT-1080) showed significant adhesion to the peptides compared to the $CD13^-$ cells (MDA-435 and MDA-231). The binding profile of the two $CD13^+$ cell lines to peptides followed a similar trend, suggesting that the binding was specific to CD13 receptor (Figure 2). The binding intensities for HT-1080 cells appeared to be slightly higher than for HUVEC cells, in contrast to expectations based on the greater expression level of CD13 on the latter. This observation is presently unexplained. The two $CD13^-$ cell lines displayed low binding to the peptide array, with MDA-MB-231 displaying slightly higher binding compared to MDA-MB-435 (Figure 2), perhaps consistent with the relative amounts of residual binding activity noted in Figure 1.

The relative cell adhesion (RCA) ratio for each peptide was calculated for the two $CD13^+$ cell lines. This allowed identification of five peptides (**5**, **14**, **21**, **22**, and **34**) that displayed higher binding compared to the other peptides. Among peptide **2**-**7**, most peptides showed enhanced binding compared to peptide **1**. Peptide **5** showed highest affinity for the cells with more than 5-fold increase in cell binding (RCA 5.4 and 5.5 for HUVEC and HT-1080, respectively) compared to peptide **1**. The peptides from group 1 (Ala scan), in general, showed good binding to the cells. Only peptide **11** with Glu8 substituted with Ala showed a relative decrease in binding (RCA 0.6) suggesting the presence of a vital electrostatic

dx.doi.org/10.1021/co300055s | *ACS Comb. Sci.* 2012, 14, 590−599

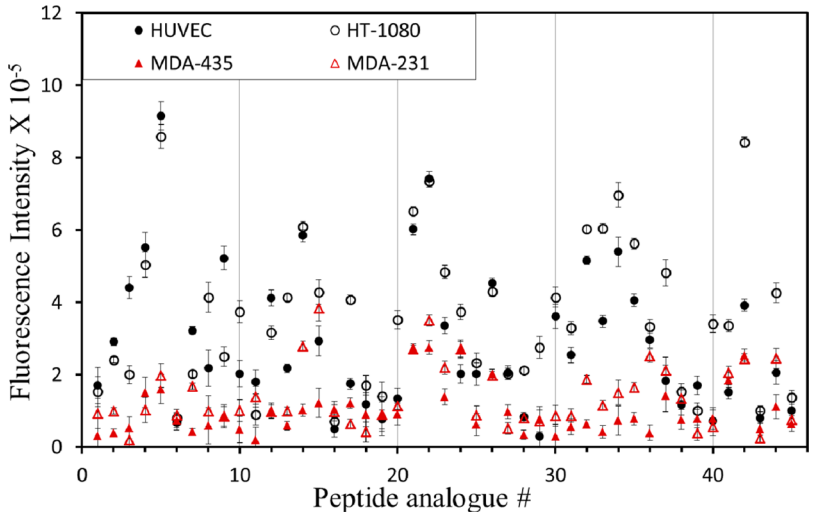

Figure 2. Average fluorescence intensity of the peptide bound cells on the cellulose membrane. Cells (75×10^3/mL), $CD13^+$ (HUVEC or HT-1080) or $CD13^-$ (MDA-231 or MDA-435), were incubated with the peptide array for 8 h at 37 °C, followed by labeling of the cells with the CyQUANT dye. The fluorescence intensity of the bound cells was measured using Kodak imager at 465 nm excitation and 535 nm emission. The results are presented as mean fluorescence intensity ± SD.

interaction with the receptor. Substitution of Val2 with Ala (peptide **8**) did not substantially change $CD13^+$ cell binding, consistent with results reported by Honda and co-workers.[41]

Peptides from group 2 with N- or C-terminal deletions showed up to 5-fold (RCA 4.8) increases in cell binding. Three peptides (**14**, **21**, and **22**) with RCA of 3 or above were selected from this group. Peptide **14** is an 8-mer with C-terminal Met deleted, whereas, peptides **21** and **22** are short peptides (5-mer and 6-mer, respectively) with mainly NGR and the two terminal cysteines for cyclization. Peptides **14** and **21** also showed low binding to $CD13^-$ cell lines. The validity of our assay was further substantiated by its identification of **21** (CNGRC), a well-known NGR peptide that has been widely used as a CD13 tumor vasculature targeting peptide;[17,42] a tumor necrosis factor-α (TNF) conjugate of this peptide is in phase II clinical trials.[18,19,24] Similarly, peptide **22** resembles the molecule cKNGRE, which has been reported to show improved binding to the $CD13^+$ cells.[28] Linear peptides **24**–**26** exhibited less cell binding compared to their cyclic analogues. Thus, cyclization of the peptide with the two terminal cysteines or the disulfide constraint is critical for the targeting efficiency, consistent with a report by Colombo et al., who found the activity of GNGRG-TNF to be 1 order of magnitude lower than that of CNGRC-TNF.[30]

Several peptides from group 3 showed augmented binding to cells compared to peptide **1**. Interestingly, substitution of NGR flanking residues with amino acids containing hydroxyl side chain, such as Ser (peptides **33** and **34**) or Thr (peptide **5**), led to increases in cell binding. Peptide **34**, with the highest RCA values (3.2 and 4.5) in group 3, was selected for further studies. Negative control peptides (**38**-**45**) mostly showed low binding to the cells (RCA $\leq$ 2.5), except for peptide **42** (RCA = 2.3 and 5.4 for the $CD13^+$ HUVEC and HT-1080 cell lines, respectively). Peptide **42** is an 8-mer linear peptide devoid of NGR sequence, which also bound both $CD13^-$ cell lines with relatively high affinity compared to other negative control sequences. Thus, this peptide was regarded as nonspecifically "sticky" to cells. Peptide **43** with RCA 0.4–0.6 was selected as a negative control peptide for further investigation.

Evaluation of In vitro Cell Binding. Peptides **5**, **14**, **21**, **22**, and **34** with enhanced binding to the $CD13^+$ cells, and peptides **1** and **43** as positive and negative controls, respectively, were chosen for in vitro cell uptake studies. These peptides were independently synthesized on 2-chlorotritylchloride resin using Fmoc-SPSS chemistry, and the N-terminus of each was labeled with FITC via a β-alanine linker (Figure S1, Supporting Information). Cyclization by disulfide bond formation was carried out by air oxidation in 20% aqueous DMSO. Buffer was not used to minimize any potential deamidation and formation of isoaspartate residue which would lead to loss in affinity for the aminopeptiase N receptor. All peptides were obtained in good yield (40–52%), and were characterized using HPLC and MALDI-TOF showing molecular ion peaks consistent with expected masses (Table 2). Peptide stock solutions were stored at neutral pH and kept at −20 °C prior to cell studies.

The soluble FITC-labeled peptides were incubated with the $CD13^+$ and $CD13^-$ cell lines for 30 min at 37 °C followed by removal of the unbound peptides by extensive washing. Cells were suspended in FACS buffer to evaluate peptide uptake by flow cytometry. The results (Figure 3) show that the NGR containing peptides **5**, **14**, **21**, **22**, and **34** were taken up

Table 2. Amino Acid Sequence and Characterization of the Peptides Selected from the Peptide Array-Whole Cell Binding Assay

no.	peptide sequence	mass[a] $[M + H]^+$ obs. (calcd)	rt (min)	yield[b] (%)
1	CVLNGRMEC	1482.5 (1482.3)	21.7	40
5	YNGRT	1071.3 (1070.4)	13.7	50
14	CVLNGREC	1351.7 (1351.2)	19.5	50
21	CNGRC	1011.1 (1010.4)	12.1	42
22	KCNGRC	1137.9 (1137.1)	11.3	45
34	CVLNGRSEC	1437.4 (1438.1)	22.2	45
43	VLGXE	990.4 (989.1)	9.5	52

[a]MALDI-TOF of FITC-β-Ala-peptide. [b]Purity of the peptides was estimated as the area under the curve of analytical HPLC chromatogram and was found to be 95–98%. r.t. = retention time.

dx.doi.org/10.1021/co300055s | ACS Comb. Sci. 2012, 14, 590–599

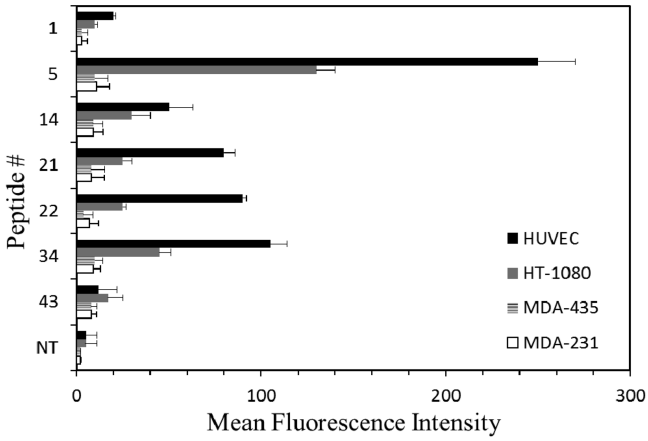

Figure 3. Peptide cell binding and uptake by $CD13^+$ and $CD13^-$ cell lines measured using flow cytometry. The peptides (10^{-6} mol/L) were incubated with the cells for 30 min at 37 °C. No treatment (NT), and FITC-**43** served as negative controls, while FITC-**1** served as a positive control. The results are presented as mean fluorescence of cell population (mean ± SD of triplicate wells).

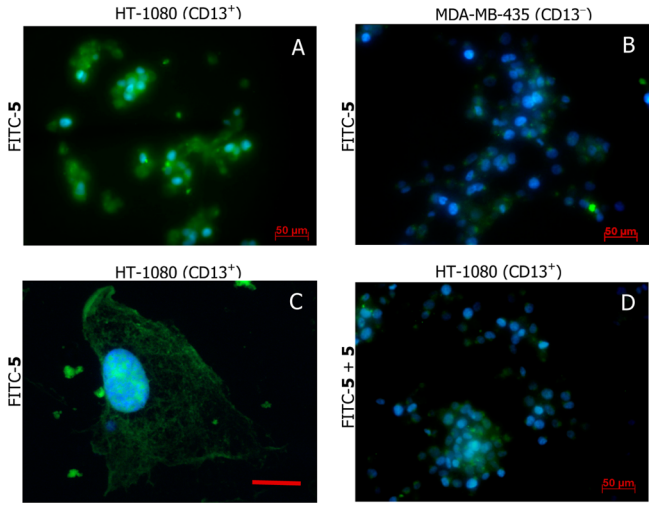

Figure 4. Fluorescence microscopy images to evaluate in vitro binding of peptide FITC-**5** to the cells. (A) HT-1080 ($CD13^+$) cells showing uptake of green FITC-**5**, (B) MDA-MB-435 ($CD13^-$) cells after incubation with FITC-**5** showing minimal uptake, (C) zoom-in of a HT-1080 cell using confocal laser microscopy showing intracellular distribution of FITC-**5** (scale bar = 12 μm), and (D) HT-1080 cells in the presence of excess unlabeled peptide **5** (10^{-4} M) as a competitor. Green, signal from FITC labeled peptide; Blue, signal from the nuclear staining agent DAPI. Images were acquired with identical exposure times and displayed consistently to compare binding between HT-1080 and MDA-MB-435 cells.

significantly more by the $CD13^+$ cell lines compared to $CD13^-$ cell lines. FITC-labeled peptide **5** (FITC-**5**) showed the highest uptake, similar to in the results of the peptide array-cell binding assay. When comparing mean cell fluorescence, the uptake of the peptides by the HUVECs was higher compared to uptake by the HT-1080 cells, in agreement with relative CD13 receptor levels determined above (Figure 1). In addition, some binding to HUVEC cells in this assay could be due to binding to $\alpha v\beta 3$ integrin receptors by NGR sequences that have converted into isoDGR under cellular conditions.[43] HT-1080 cancer cells do not express $\alpha v\beta 3$ integrins.[44]

Peptide **5**, a linear 5-mer sequence, was further evaluated for cellular uptake. Fluorescence microscopy images (Figure 4A) of $CD13^+$ HT-1080 cells showed strong intersperse fluorescence, while the $CD13^-$ MD-435 cells showed much less green fluorescence (Figure 4B) demonstrating peptide specificity for the APN/CD13 receptor. Figure 4C shows zoomed-in image of the HT-1080 cells, where uniform distribution of FITC-**5** peptide inside the cell and nucleus is observed. The binding of the FITC-**5** peptide was inhibited to a large extent in the presence of 100-fold excess unlabeled peptide **5** (Figure 4D). Finally, a coculture assay with HT-1080 and MDA-MB-435 cells was performed to study the selectivity of peptide FITC-**5**. $CD13^+$ HT-1080 cells were grown together with the $CD13^-$ MDA-MB-435 cells followed by incubation with FITC-**5**. As shown in Figure 5, MDA-MB-435 cells, previously stained with blue cell tracker dye, showed much less green fluorescence due to peptide uptake compared to the HT-1080 cells.

As noted above, the residual uptake of the peptide by the MDA-MB-435 cells (Figures 4B and 5B) could be due to the binding of isoDGR peptide of FITC-**5** to the $\alpha v\beta 3$ integrin expressed by these cells.[39] To investigate the susceptibility of peptides toward deamination under condition used in the binding assays, we studied the stability of peptide **5**, a representative NGR sequence, in DMEM media at 37 °C, assaying by MALDI-TOF mass spectrometry and RP-HPLC (Supporting Information Figure S4). The peptide started to disintegrate after 4 h incubation as evidenced by the appearance of multiple peaks during HPLC and mass analysis. Mass measurement indicated the presence of NGR peptide, deaminated *iso*DGR or DGR, and a succinamide intermediate at m/z values of 610.7 ($[M+H]^+$), 611.7 (+1), and 593.5 (−17), respectively (Supporting Information Figure S4B and S4C). These results suggest that the NGR sequence was maintained during the half-hour period of the in vitro binding assays with cells in DMEM media. The peptide was found to be completely stable in water for extended periods under similar conditions.

Inhibition of Aminopeptidase N Activity by Selected Peptides. Inhibition of APN enzyme is considered important as it inhibits tumor invasion and angiogenesis causing tumor regression.[45] We examined the ability of five most promising NGR peptides and peptide **1** to inhibit aminopeptidase N activity, with bestatin as a positive control.[46] Screening of peptides for inhibition of APN activity was carried out at a single substrate concentration of 500 μM for 30 min, as lower concentrations (125 μM or lower) did not show noticeable activity (Figure 6). Peptide **5** was the most potent, causing 60 ± 4.2% inhibition compared to 92% inhibition by bestatin. Peptide **34** showed 54 ± 3.9% inhibition, suggesting again the importance of hydroxyl side chain group in enhancing binding and interaction with $CD13^+$ cells or the APN enzyme. Peptides **1**, **14**, **21**, and **22** displayed little to no inhibition (<20%) at the tested concentration. Previously it has been reported that CNGRC peptide showed minimal inhibition of APN up to 500 μM concentration.[23] A recently identified CPNGRC peptide sequence showed that the addition of a proline residue enhanced binding to the APN enzyme as well as inhibited APN proteolytic activity with an IC50 of 10 μM, a value that is 30-fold lower than that for CNGRC.[31] Along with these precedents, this study highlights the possible correlation between enhanced binding to APN and APN inhibition.

The YNGRT sequence (peptide **5**) is present in the type II module of fibronectin.[39] The three-dimensional (3D) structure of peptide **5** excised from the fibronectin structure (PDB

dx.doi.org/10.1021/co300055s | ACS Comb. Sci. 2012, 14, 590−599

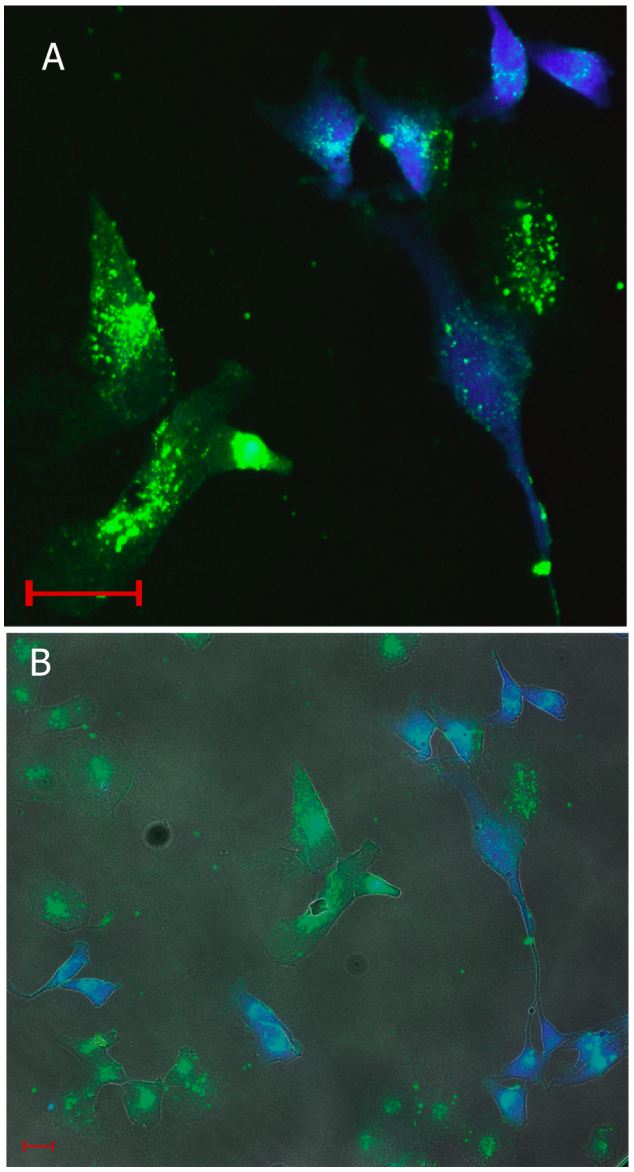

Figure 5. (A) Fluorescence microscopy image of a coculture of HT-1080 ($CD13^+$) and MDA-MB-435 ($CD13^-$) cells incubated with FITC-**5** (green) for 30 min. Peptide (green) was uptaken primarily by HT-1080 cells with very little uptake by MDA-MB-435 cells. The MDA-MB-435 cells were stained blue using cell tracker blue before the experiment. (B) A phase contrast image. Scale bar = 20 μm.

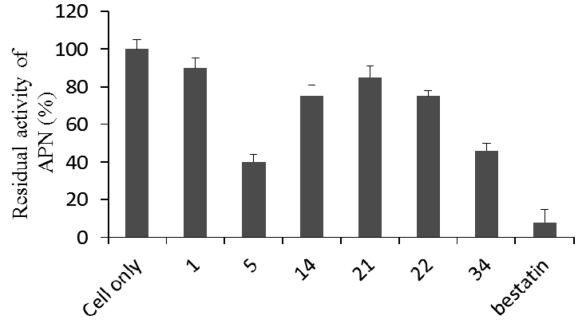

Figure 6. Inhibition of aminopeptidase N (APN) activity in the presence of NGR peptides. Intact HT-1080 cells were incubated with peptides or bestatin (a known inhibitor) followed by evaluation of APN activity. The results shown are mean ± SD of triplicates.

1QO6)[47] is shown in Figure 7. An overlay of peptide **5** with LNGRS sequence of peptide **34** (derived from PDB 3NWJ)[48] shows that peptide **34** may also fold into similar conformation. The structures discussed here represent possible solution conformations of the individual peptides as these structures are based on the structure of the peptide in a complete protein. The true 3D structures of peptides, such as **5** and **34** remain to be elucidated. The other high affinity peptides also resemble sequences from fibronectin. Peptides **21** and **22** contain CNGRC which has been shown to be a better analogue of fibronectin sequence GNGRG (Figure 7).[30] GNGRG belongs to the type I module (5th and seventh type I repeats) of fibronectin (PDB 1FBR)[49] and the cyclized CNGRC stabilizes the linear sequence providing higher affinity for CD13.[30] Peptide **14** contains LNGRE sequence which is present in the type III module of fibronectin (PDB 1FNF).[50] Thus, all the high affinity peptides identified in the present study are derivatives of the fibronectin NGR sequences.

CONCLUSIONS

Peptide-array cell binding assay using cellulose bound peptides was able to screen for cyclic and acyclic NGR peptides that bind to $CD13^+$ cell lines. Membrane cell binding results, as well as in vitro binding experiments including coculture fluorescence microscopy suggest that the identified NGR peptides bind selectively to CD13 receptor in $CD13^+$ cell lines. Interestingly, peptide **21** (CNGRC) identified here is a well-known NGR peptide that has been widely used as a CD13 tumor vasculature targeting peptide.[18] The newly identified sequences presented in this study, such as peptides **5** and **34**, offer additional advantages to the previously reported NGR sequence. Peptide **5** (YNGRT), the most promising peptide identified, showed a significant increase (up to 13-fold) in uptake by the $CD13^+$ cells compared to the lead peptide **1**. Peptide **5** is a linear peptide that can be cyclized to further enhance its binding properties toward $CD13^+$ cells. In addition, the new sequences, such as **5** and **34**, display better APN enzyme inhibition and selectivity toward $CD13^+$ cells.

In conclusion, the NGR peptides identified here are promising sequences for developing tumor vasculature targeted drugs, delivery systems and imaging agents with reduced detrimental off-target effects from the toxic drug or other agents. Our results show that peptide array library screening is a powerful research tool for analyzing peptide-cell interactions with rapid and efficient screening of high binding peptides. Both cyclic and linear peptides containing NGR were identified that closely resemble NGR sequences present in human fibronectin. Consequently, these NGR sequences may have low immunogenicity making them ideal candidates for the development of ligands for targeted delivery to tumor angiogenic vasculature.

EXPERIMENTAL PROCEDURES

Peptide Array Synthesis. Peptide array consisting of forty five peptide sequences (ranging from 5-mer to 9-mer) in duplicates was synthesized on a cellulose membrane using an AutoSpot as described previously.[33] Briefly, peptide array was synthesized on an amino-PEG500 cellulose membrane derivatized with a polyethylene (PEG) spacer and a free amino terminal group using a semiautomatic robot AutoSpot ASP222 (Intavis AG, Germany). DIGEN software (Jerini Biotools GmbH, Berlin, Germany) was used for formatting the

dx.doi.org/10.1021/co300055s | ACS Comb. Sci. 2012, 14, 590−599

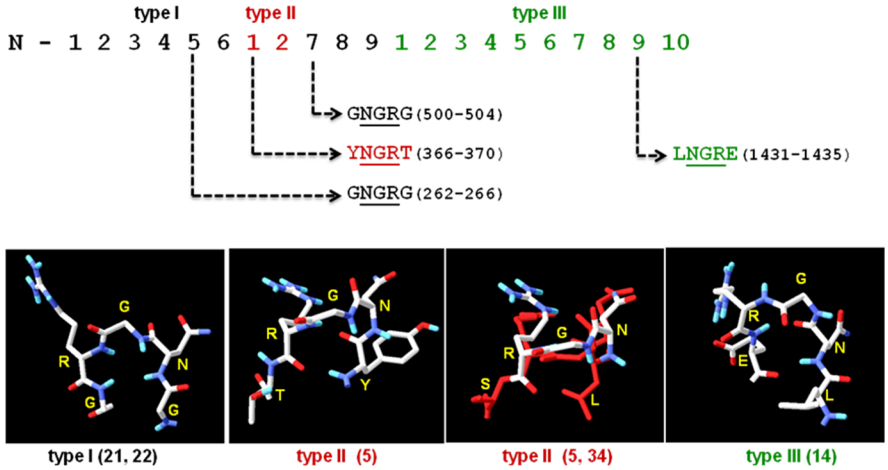

Figure 7. Schematic representation of a portion of human fibronectin highlighting NGR motifs present in the type I, II, and III repeats (top). Three dimensional structures of the NGR sequences present in the type I (PDB 1FBR), II (PDB 1QO6), and III (PDB 1FNF) repeats are shown as stick models (bottom). Peptides **21** and **22** most likely form hairpin as found in type I structure (bottom, left to right), peptide **5** folds into type II structure, and peptide **34** which is similar to peptide **5** may form type II structure. An overlay of peptide **5** with type II fold and peptide **34** (red) derived from PDB 3NWJ is shown. LNGRE of type III repeat, which is present in peptide **14**, is also shown.

array. The synthesis was started by anchoring a β-alanine residue (linker) to the cellulose membrane and thereafter peptides were synthesized from the C-terminal end. Fmoc amino acids (0.25 mM/mL) activated with HOBt and DIC were spotted on the membrane in 60 nL aliquots per spot by a robotic syringe, yielding a peptide loading of 0.4 μmol/cm^2. After coupling of the Fmoc amino acid, the membrane was removed from the synthesizer and was treated with acetic anhydride (2%) to cap any free remaining amino groups. Piperidine (20%) in DMF was used for Fmoc deprotection. After it was washed, the membrane was air-dried and carefully repositioned on the robotic synthesizer to repeat the coupling cycles to complete the peptide sequence. At the end, all peptides were N-terminally acetylated. The final removal of side chain protecting groups was performed by treating the membrane with a cocktail of reagents, comprised of TFA (15 mL), DCM (15 mL), triisopropylsilane (0.9 mL), and water (0.6 mL), for about 3 h. After extensive washing with DCM, DMF, and ethanol, the membrane was dried with cold air. Next, the cyclization of cysteine containing peptides was performed to form the disulfide bond. The membrane was incubated with 20% DMSO in water for 24 h at 4 °C, and finally overnight at rt. Subsequently, the membrane was washed with ethanol (3 × 3 min), dried, and stored in a sealed bag at −20 °C until use. To ensure cyclization on the membrane, we have previously characterized representative cyclic peptides using a membrane with a cleavable linker.[33] For membrane regeneration, the bound cells were removed after each cell-binding experiment by first washing with ethanol for 5 min, followed by treatment with 0.1 N HCl for 20 min. The peptide array membrane was then washed with DMF (4 × 20 min), ethanol (3 × 3 min), and finally dried in air.

APN/CD13 Expression Level Using FACS Analysis. Fluorescence activated cell sorting (FACS) was performed to quantify the level of expression of APN/CD13 among the selected four cell lines. The human fibrosarcoma HT-1080 (American Type Culture Collection, Manassas, VA) and the human breast cancer cell line MDA-MB-231 were cultured in DMEM with Glutamax containing 10% FCS (Invitrogen). Human umbilical vein endothelial cells (HUVEC) were kind gift from the laboratory of Sandra Davidge, University of Alberta. These cells were cultivated using Endothelial Cell Growth Medium (EGM, LONZA) containing 20% FCS, 2 mmol/L glutamine, 100 IU/mL penicillin, 100 IU/mL streptomycin, and 2 ng/mL basic fibroblast growth factor (Roche Diagnostics, Mannheim, Germany). The human cancer cell line MDA-MB-435 was cultured in RPMI-1640 with Glutamax containing 10% FCS (Invitrogen, Karlsruhe, Germany), 100 IU/mL penicillin, and 100 IU/mL streptomycin. All cell lines were cultured at 37 °C in a 5% CO_2 incubator. Cells (10^6) were suspended in FACS buffer (100 μL, PBS with 2% FCS), and incubated with FITC labeled CD13 antihuman antibody (20 μL, WM-15) for 30 min at 4 °C. The cells were washed twice with FACS buffer after centrifugation, the same was done for cells without antibody treatment which served as a negative control, and the APN/CD13 expression level was measured using flow cytometry. FACS experiments were performed on a Beckman Coulter QUANTA SC Flow Cytometer. The data was analyzed by CellQuest software and is presented as the average of mean cell fluorescence intensity (±SD) of triplicate wells.

Peptide Array-Cell Binding Assay. Peptide array-whole cell binding was performed following the method developed in our laboratory previously.[33] Briefly, the peptide array membrane was incubated with the cells (20 mL, 75 × 10^3 cells/mL) for 8 h in serum free media. After washing the nonbound cells, the membrane was first frozen at −80 °C for 2 h followed by thawing at r.t. and incubation with the CyQUANT dye. The membrane was washed (6× with PBS) and scanned using Kodak imager (λ_{ex} 465 nm, λ_{em} 535 nm). The net fluorescence intensity of each peptide spot was quantified using Kodak Molecular Imaging Software Version 4.0. An external standard peptide was used to calibrate the fluorescence intensity between scans performed on the same day and on different days. The membrane was regenerated after each cell-binding experiment. Each cell-binding experiment was repeated twice for the four cell lines. The results are presented as average fluorescence intensity (±standard deviation) of two duplicate peptide spots, two scans, and two different experiments. The relative cell adhesion ratio (Table 1) for each peptide sequence was calculated as the ratio of the average

dx.doi.org/10.1021/co300055s | ACS Comb. Sci. 2012, 14, 590−599

fluorescence of the peptide analogue divided by that of parent peptide **1**.

Synthesis of FITC-Labeled Peptides. Seven FITC-labeled peptides, (FITC-**1**, FITC-**5**, FITC-**14**, FITC-**21**, FITC-**22**, FITC-**34**, FITC-**43**), and two unlabeled peptides (**1** and **22**) were synthesized on an automatic synthesizer (Advanced ChemTech MPS 357, Louisville, KY, USA) following Fmoc solid phase peptide synthesis (SPPS).[51] Peptides were synthesized on 2-chlorotritylchloride resin (0.1 mmol, 1 mmol/g) using DIC/HOBT mixture as coupling agent. After complete peptide synthesis, β-alanine was conjugated to the N-terminal amino group followed by fluorescein isothiocyanate (FITC) coupling. FITC (0.3 mmol) was coupled to peptide using DIPEA (0.6 mmol) in dark for 24 h, followed by extensive washing of the resin. FITC-labeled peptide was cleaved from the resin, along with the deprotection of the amino acid side chains by TFA/DCM (50:50) mixture. The crude cleaved peptides were precipitated by cold diethyl ether followed by their purification using RP-HPLC. Peptide oxidation was carried out by incubating peptide in 20% aqueous DMSO solution at pH 7 (r.t., 2 days). Disulfide bond formation was confirmed with Ellman test and MALDI-TOF mass spectrometry. The peptides were purified by RP-HPLC (Varian Prostar HPLC, Walkersville, MD, USA) using a linear gradient of isopropranol/water containing 0.1% TFA and were lyophilized. Purity of the final products was analyzed using analytical RP-HPLC (Supporting Information Figure S3) and MALDI-TOF mass characterization (Table 2 and Supporting Information Figure S2). Stock solution for the peptides was prepared in sterile 10% aqueous acetonitrile and stored at −20 °C. Peptide concentrations were determined by measuring fluorescence at excitation 465 nm and emission 535 nm.

Peptide Stability and Deamination. To evaluate peptide stability, a solution of peptide **5** in DMEM was incubated at 37 °C, mimicking conditions used in the in vitro cell binding experiments. At different time intervals, aliquots were removed and peptide stability was monitored using MALDI-TOF mass spectrometry and RP-HPLC. The same experiment was also repeated for peptide in water.

In Vitro Cellular Uptake Using FACS. FACS analysis was used to evaluate the binding of the FITC-labeled peptides to $CD13^+$ (HUVEC and HT-1080) and $CD13^-$ (MDA-MB-435 and MDA-MB-231) cell lines. Cells were placed into 6-well plates at a density of 10^6 in culture media (3 mL) at 37 °C for 24 h to adhere to the plate surface. The culture media was replaced with fresh serum-free media (1 mL) containing FITC-labeled peptides at a concentration of 10^{-6} mol/L. Cells were incubated with the peptides for 30 min at 37 °C. The media was then removed and the cells were washed to remove the unbound peptides. The cells were scrapped and transferred to centrifuge tubes followed by centrifugation at 1000 rpm for 7 min. The pellet was resuspended in FACS buffer (2% FCS in PBS), washed once more and then resuspended again in FACS buffer. Untreated cells were subjected to similar steps to detect autofluorescence of the cells. The samples were then subjected to the FACS instrument, Beckman Coulter QUANTA SC Flow Cytometer using the FL1 channel (10 000 events/sample). Instrument settings were calibrated so that untreated cells show 1−2% of fluorescence. The mean cell fluorescence was determined (λ_{ex} 485 nm, λ_{em} 525 nm) and the data was analyzed by Quanta SC software.

Cellular Uptake using Fluorescence Microscopy. MDA-MB-435 or HUVEC cells (50 000) were cultured on the top of a coverslip at 37 °C for 24 h. The medium was removed and replaced with fresh serum free medium (1 mL), containing FITC-**5** (10^{-6} mol/L). The cells were incubated with the peptide for 30 min at 37 °C. After incubation, the medium was removed and the cells were washed with serum free medium (3 × 2 mL). The cells were fixed on ice with 2% formaldehyde for 20 min. The formaldehyde was removed by washing with media (3 times). The coverslips were put on slides containing one drop of DAPI-Antifade (Molecular Probes) to stain the nucleus. The cells were imaged under the fluorescence microscope (Zeiss, Göttingen, Germany) using green and blue filters with 20× magnification. The samples prepared for fluorescence microscopy were also used for visualization by confocal microscopy. Confocal laser scanning microscopy was performed with a Zeiss 510 LSMNLO confocal microscope (Carl Zeiss Microscope Systems, Jena, Germany) with a 40× oil immersion lens. For the competitive binding, the same experiment was carried out in the presence of unlabeled peptide **5** (10^{-4} mol/L) as a competitor.

A coculture experiment of HT-1080 and MDA-MB-435 cells was carried out as previously described.[52] Briefly, to visualize the cells and distinguish between HT-1080 and MDA-MB-435 cells in the coculture, adherent MDA-435 cells were stained using the Blue Cell Tracker fluorescent dye (25 μM) according to the manufacturer's protocol. MDA-MB-435 cells were incubated with dye in serum free media at 37 °C for 35 min, followed by another 30 min in fresh media. Subsequently, HT-1080 and MDA-MB-435 cells were cultured together in a 24-well plate with coverslip at a density of 2×10^5 cells/well for 24 h at 37 °C, and the seeding ratio was 1:1. The following day, cells were incubated with FITC-**5** (10 μM) in DMEM serum free media for 30 min at 37 °C. After they were washed with PBS (3 times), cells were fixed using 2% formaldehyde in PBS for 20 min on ice, and the coverslip was placed onto a glass slide over the fluorescence mounting medium. The images were acquired by a fluorescence microscope at 20× magnification with FITC and DAPI filters.

Aminopeptidase Enzymatic Inhibition. APN activity on the surface of intact HT-1080 cells was measured using Ala-4-nitroanilide (H·Ala-pNA·HCl) as a substrate, and bestatin as a specific inhibitor (positive control). Experiment was carried out as previously described with some modifications.[46] In a typical experiment, cells (2×10^5) were seeded in each well of a 24-well culture plate, and after incubation for 24 h at 37 °C, media was aspirated. The cells were preincubated for 5 min with peptide or bestatin at 0.5 mM concentration in PBS (pH 7.4). Following which, Ala-pNA substrate (6 mM) at 37 °C was added directly, and further incubated in the dark for 30 min at 37 °C. The supernatant from each well was collected, centrifuged, and enzyme activity was determined by measuring formation of yellow pNA at 405 nm using a Power Wave X340 microplate reader (Bio-Tek Instrument Inc. USA). To quantify the effect of inhibitors, the remaining activity was expressed as the percentage of the control activity without inhibitor. All measurements were made in triplicates.

■ ASSOCIATED CONTENT

Ⓢ Supporting Information

Additional figures (S1−S4) related to peptide synthesis, purification, characterization, and stability. This material is available free of charge via the Internet at http://pubs.acs.org.

dx.doi.org/10.1021/co300055s | ACS Comb. Sci. 2012, 14, 590−599

AUTHOR INFORMATION

Corresponding Author

*Tel.: 780-492-8917. Fax: 780-492-1217. E-mail: kkaur@ualberta.ca.

Notes

The authors declare no competing financial interest.

ACKNOWLEDGMENTS

We dedicate this manuscript to late Dr. John Samuel. We thank Haitham El-Sikhry for assistance in acquiring Figure 5 microscopy image. This work was supported by the Natural Sciences and Engineering Research Council of Canada (NSERC). The infrastructure support from the Canada Foundation for Innovation (CFI) is also acknowledged. R.S. is the recipient of the Egyptian Government Scholarship.

ABBREVIATIONS

aa, amino acid; APN, aminopeptidase N; DCM, dichloromethane; DIC, *N,N′*-diisopropylcarbodiimide; DMF, *N,N*-dimethylformamide; FACS, fluorescence activated cell sorting; FITC, fluorescein isothiocyanate; FN, fibronectin; HOBt, 1-hydroxybenzotriazole; MALDI-TOF, matrix-assisted laser desorption ionization time-of-flight spectrometry; NMM, *N*-methyl morpholine; RCA, relative cell adhesion ratio; RP-HPLC, reversed-phase HPLC; rt, room temperature; TFA, trifluoroacetic acid

REFERENCES

(1) Ruoslahti, E.; Bhatia, S. N.; Sailor, M. J. Targeting of drugs and nanoparticles to tumors. *J. Cell Biol.* **2010**, *188*, 759−768.

(2) Liu, Z.; Wu, K. Peptides homing to tumor vasculature: Imaging and therapeutics for cancer. *Recent Pat. Anti-Cancer Drug Discovery* **2008**, *3*, 202−208.

(3) Chen, K.; Chen, X. Integrin targeted delivery of chemotherapeutics. *Theranostics* **2011**, *1*, 189−200.

(4) Brooks, P. C.; Clark, R. A. F.; Cheresh, D. A. Requirement of vascular integrin alpha v beta 3 for angiogenesis. *Science* **1994**, *264*, 569−571.

(5) Wickström, M.; Larsson, R.; Nygren, P.; Gullbo, J. Aminopeptidase N (CD13) as a target for cancer chemotherapy. *Cancer Sci.* **2011**, *102*, 501−508.

(6) Hicklin, D. J.; Ellis, L. M. Role of the vascular endothelial growth factor pathway in tumor growth and angiogenesis. *J. Clin. Oncol.* **2005**, *23*, 1011−1027.

(7) Veikkola, T.; Karkkainen, M.; Claesson-Welsh, L.; Alitalo, K. Regulation of angiogenesis via vascular endothelial growth factor receptors. *Cancer Res.* **2000**, *60*, 203−212.

(8) Silletti, S.; Kessler, T.; Goldberg, J.; Boger, D. L.; Cheresh, D. A. Disruption of matrix metalloproteinase 2 binding to integrin $\alpha v\beta 3$ by an organic molecule inhibits angiogenesis and tumor growth in vivo. *Proc. Natl. Acad. Sci.* **2001**, *98*, 119−124.

(9) Desgrosellier, J. S.; Cheresh, D. A. Integrins in cancer: Biological implications and therapeutic opportunities. *Nat. Rev. Cancer* **2010**, *10*, 9−22.

(10) Allen, T. M. Ligand-targeted therapeutics in anticancer therapy. *Nat. Rev. Cancer* **2002**, *2*, 750−763.

(11) Mina-Osorio, P. The moonlighting enzyme CD13: Old and new functions to target. *Trends Mol. Med.* **2008**, *14*, 361−371.

(12) Fukasawa, K.; Fujii, H.; Saitoh, Y.; Koizumi, K.; Aozuka, Y.; Sekine, K.; Yamada, M.; Saiki, I.; Nishikawa, K. Aminopeptidase N (APN/CD13) is selectively expressed in vascular endothelial cells and plays multiple roles in angiogenesis. *Cancer Lett.* **2006**, *243*, 135−143.

(13) Curnis, F.; Arrigoni, G.; Sacchi, A.; Fischetti, L.; Arap, W.; Pasqualini, R.; Corti, A. Differential binding of drugs containing the NGR Motif to CD13 isoforms in tumor vessels, epithelia, and myeloid cells. *Cancer Res.* **2002**, *62*, 867−874.

(14) Matteo, P. D.; Arrigoni, G. L.; Alberici, L.; Corti, A.; Gallo-Stampino, C.; Traversari, C.; Doglioni, C.; Rizzardi, G.-P. Enhanced expression of CD13 in vessels of inflammatory and neoplastic tissues. *J. Histochem. Cytochem.* **2011**, *59*, 47−59.

(15) Pasqualini, R.; Koivunen, E.; Kain, R.; Lahdenranta, J.; Sakamoto, M.; Stryhn, A.; Ashmun, R. A.; Shapiro, L. H.; Arap, W.; Ruoslahti, E. Aminopeptidase N is a receptor for tumor-homing peptides and a target for inhibiting angiogenesis. *Cancer Res.* **2000**, *60*, 722−727.

(16) Pasqualini, R.; Koivunen, E.; Ruoslahti, E. A peptide isolated from phage display libraries is a structural and functional mimic of an RGD-binding site on integrins. *J. Cell Biol.* **1995**, *130*, 1189−1196.

(17) Arap, W.; Pasqualini, R.; Ruoslahti, E. Cancer treatment by targeted drug delivery to tumor vasculature in a mouse model. *Science* **1998**, *279*, 377−380.

(18) Curnis, F.; Sacchi, A.; Borgna, L.; Magni, F.; Gasparri, A.; Corti, A. Enhancement of tumor necrosis factor [alpha] antitumor immunotherapeutic properties by targeted delivery to aminopeptidase N (CD13). *Nat. Biotechnol.* **2000**, *18*, 1185−1190.

(19) Grifman, M.; Trepel, M.; Speece, P.; Gilbert, L. B.; Arap, W.; Pasqualini, R.; Weitzman, M. D. Incorporation of tumor-targeting peptides into recombinant adeno-associated virus capsids. *Mol. Ther.* **2001**, *3*, 964−975.

(20) Pastorino, F.; Brignole, C.; Marimpietri, D.; Cilli, M.; Gambini, C.; Ribatti, D.; Longhi, R.; Allen, T. M.; Corti, A.; Ponzoni, M. Vascular damage and anti-angiogenic effects of tumor vessel-targeted liposomal chemotherapy. *Cancer Res.* **2003**, *63*, 7400−7409.

(21) Di Matteo, P.; Curnis, F.; Longhi, R.; Colombo, G.; Sacchi, A.; Crippa, L.; Protti, M. P.; Ponzoni, M.; Toma, S.; Corti, A. Immunogenic and structural properties of the Asn-Gly-Arg (NGR) tumor neovasculature-homing motif. *Mol. Immunol.* **2006**, *43*, 1509−1518.

(22) Corti, A.; Curnis, F.; Arap, W.; Pasqualini, R. The neovasculature homing motif NGR: More than meets the eye. *Blood* **2008**, *112*, 2628−2635.

(23) van Hensbergen, Y.; Broxterman, H. J.; Elderkamp, Y. W.; Lankelma, J.; Beers, J. C. C.; Heijn, M.; Boven, E.; Hoekman, K.; Pinedo, H. M. A doxorubicin−CNGRC−peptide conjugate with prodrug properties. *Biochem. Pharmacol.* **2002**, *63*, 897−908.

(24) Ndinguri, M. W.; Solipuram, R.; Gambrell, R. P.; Aggarwal, S.; Hammer, R. P. Peptide targeting of platinum anti-cancer drugs. *Bioconjug. Chem.* **2009**, *20*, 1869−1878.

(25) Ellerby, H. M.; Arap, W.; Ellerby, L. M.; Kain, R.; Andrusiak, R.; Rio, G. D.; Krajewski, S.; Lombardo, C. R.; Rao, R.; Ruoslahti, E.; Bredesen, D. E.; Pasqualini, R. Anti-cancer activity of targeted pro-apoptotic peptides. *Nat. Med.* **1999**, *5*, 1032−1038.

(26) Santoro, A.; Pressiani, T.; Citterio, G.; Rossoni, G.; Donadoni, G.; Pozzi, F.; Rimassa, L.; Personeni, N.; Bozzarelli, S.; Colombi, S.; De Braud, F. G.; Caligaris-Cappio, F.; Lambiase, A.; Bordignon, C. Activity and safety of NGR-hTNF, a selective vascular-targeting agent, in previously treated patients with advanced hepatocellular carcinoma. *Br. J. Cancer* **2010**, *103*, 837−844.

(27) Santoro, A.; Rimassa, L.; Sobrero, A. F.; Citterio, G.; Sclafani, F.; Carnaghi, C.; Pessino, A.; Caprioni, F.; Andretta, V.; Tronconi, M. C.; Finocchiaro, G.; Rossoni, G.; Zanoni, A.; Miggiano, C.; Rizzardi, G.-P.; Traversari, C.; Caligaris-Cappio, F.; Lambiase, A.; Bordignon, C. Phase II study of NGR-hTNF, a selective vascular targeting agent, in patients with metastatic colorectal cancer after failure of standard therapy. *Eur. J. Cancer* **2010**, *46*, 2746−2752.

(28) Negussie, A. H.; Miller, J. L.; Reddy, G.; Drake, S. K.; Wood, B. J.; Dreher, M. R. Synthesis and in vitro evaluation of cyclic NGR peptide targeted thermally sensitive liposome. *J. Controlled Release* **2010**, *143*, 265−273.

(29) Metaferia, B. B.; Rittler, M.; Gheeya, J. S.; Lee, A.; Hempel, H.; Plaza, A.; Stetler-Stevenson, W. G.; Bewley, C. A.; Khan, J. Synthesis of novel cyclic NGR/RGD peptide analogs via on resin click chemistry. *Bioorg. Med. Chem. Lett.* **2010**, *20*, 7337−7340.

(30) Colombo, G.; Curnis, F.; De Mori, G. M. S.; Gasparri, A.; Longoni, C.; Sacchi, A.; Longhi, R.; Corti, A. Structure−activity relationships of linear and cyclic peptides containing the NGR tumor-homing motif. *J. Biol. Chem.* **2002**, *277*, 47891−47897.
(31) Plesniak, L. A.; Salzameda, B.; Hinderberger, H.; Regan, E.; Kahn, J.; Mills, S. A.; Teriete, P.; Yao, Y.; Jennings, P.; Marassi, F.; Adams, J. A. Structure and activity of CPNGRC: A modified CD13/APN peptidic homing motif. *Chem. Biol. Drug Des.* **2010**, *75*, 551−562.
(32) Curnis, F.; Cattaneo, A.; Longhi, R.; Sacchi, A.; Gasparri, A. M.; Pastorino, F.; Di Matteo, P.; Traversari, C.; Bachi, A.; Ponzoni, M.; Rizzardi, G.-P.; Corti, A. Critical Role of Flanking Residues in NGR-to-isoDGR transition and CD13/integrin receptor switching. *J. Biol. Chem.* **2010**, *285*, 9114−9123.
(33) Ahmed, S.; Mathews, A. S.; Byeon, N.; Lavasanifar, A.; Kaur, K. Peptide Arrays for Screening Cancer Specific Peptides. *Anal. Chem.* **2010**, *82*, 7533−7541.
(34) Hwang, R.; Varner, J. The role of integrins in tumor angiogenesis. *Hematol. Oncol. Clin. North Am.* **2004**, *18*, 991−1006.
(35) Haubner, R.; Weber, W. A.; Beer, A. J.; Vabuliene, E.; Reim, D.; Sarbia, M.; Becker, K.-F.; Goebel, M.; Hein, R.; Wester, H.-J.; Kessler, H.; Schwaiger, M. Noninvasive visualization of the activated $\alpha v\beta 3$ integrin in cancer patients by positron emission tomography and [18F]galacto-RGD. *PLoS Med.* **2005**, *2*, e70.
(36) Sugahara, K. N.; Teesalu, T.; Karmali, P. P.; Kotamraju, V. R.; Agemy, L.; Greenwald, D. R.; Ruoslahti, E. Coadministration of a tumor-penetrating peptide enhances the efficacy of cancer drugs. *Science* **2010**, *328*, 1031−1035.
(37) Koivunen, E.; Gay, D. A.; Ruoslahti, E. Selection of peptides binding to the alpha 5 beta 1 integrin from phage display library. *J. Biol. Chem.* **1993**, *268*, 20205−20210.
(38) Lau, D. H.; Guo, L.; Liu, R.; Song, A.; Shao, C.; Lam, K. S. Identifying peptide ligands for cell surface receptors using cell-growth-on-bead assay and one-bead one-compound combinatorial library. *Biotechnol. Lett.* **2002**, *24*, 497−500.
(39) Curnis, F.; Longhi, R.; Crippa, L.; Cattaneo, A.; Dondossola, E.; Bachi, A.; Corti, A. Spontaneous formation of L-isoaspartate and gain of function in fibronectin. *J. Biol. Chem.* **2006**, *281*, 36466−36476.
(40) Shim, J. S.; Kim, J. H.; Cho, H. Y.; Yum, Y. N.; Kim, S. H.; Park, H.-J.; Shim, B. S.; Choi, S. H.; Kwon, H. J. Irreversible inhibition of CD13/aminopeptidase N by the antiangiogenic agent curcumin. *Chem. Biol.* **2003**, *10*, 695−704.
(41) Okochi, M.; Nomura, S.; Kaga, C.; Honda, H. Peptide array-based screening of human mesenchymal stem cell-adhesive peptides derived from fibronectin type III domain. *Biochem. Biophys. Res. Commun.* **2008**, *371*, 85−89.
(42) Jiang, W.; Jin, G.; Ma, D.; Wang, F.; Fu, T.; Chen, X.; Chen, X.; Jia, K.; Marikar, F. M.; Hua, Z. Modification of cyclic NGR tumor neovasculature-homing motif sequence to human plasminogen kringle 5 improves inhibition of tumor growth. *PLoS One* **2012**, *7*, e37132.
(43) Spitaleri, A.; Mari, S.; Curnis, F.; Traversari, C.; Longhi, R.; Bordignon, C.; Corti, A.; Rizzardi, G.-P.; Musco, G. Structural basis for the interaction of isoDGR with the RGD-binding Site of $\alpha v\beta 3$ integrin. *J. Biol. Chem.* **2008**, *283*, 19757−19768.
(44) Berditchevski, F.; Zutter, M. M.; Hemler, M. E. Characterization of novel complexes on the cell surface between integrins and proteins with 4 transmembrane domains (TM4 proteins). *Mol. Biol. Cell* **1996**, *7*, 193−207.
(45) Aozuka, Y.; Koizumi, K.; Saitoh, Y.; Ueda, Y.; Sakurai, H.; Saiki, I. Anti-tumor angiogenesis effect of aminopeptidase inhibitor bestatin against B16−BL6 melanoma cells orthotopically implanted into syngeneic mice. *Cancer Lett.* **2004**, *216*, 35−42.
(46) Bauvois, B.; Puiffe, M.-L.; Bongui, J.-B.; Paillat, S.; Monneret, C.; Dauzonne, D. Synthesis and biological evaluation of novel flavone-8-acetic acid derivatives as reversible inhibitors of aminopeptidase N/CD13. *J. Med. Chem.* **2003**, *46*, 3900−3913.
(47) Bocquier, A. A.; Potts, J. R.; Pickford, A. R.; Campbell, I. D. Solution structure of a pair of modules from the gelatin-binding domain of fibronectin. *Structure* **1999**, *7*, 1451−S3.
(48) Fucile, G.; Garcia, C.; Carlsson, J.; Sunnerhagen, M.; Christendat, D. Structural and biochemical investigation of two *Arabidopsis shikimate* kinases: The heat-inducible isoform is thermostable. *Protein Sci.* **2011**, *20*, 1125−1136.
(49) Williams, M. J.; Phan, I.; Harvey, T. S.; Rostagno, A.; Gold, L. I.; Campbell, I. D. Solution structure of a pair of fibronectin type 1 modules with fibrin binding activity. *J. Mol. Biol.* **1994**, *235*, 1302−1311.
(50) Leahy, D. J.; Aukhil, I.; Erickson, H. P. 2.0 Å Crystal structure of a four-domain segment of human fibronectin encompassing the RGD loop and synergy region. *Cell* **1996**, *84*, 155−164.
(51) Soliman, W.; Wang, L.; Bhattacharjee, S.; Kaur, K. Structure−activity relationships of an antimicrobial peptide plantaricin S from two-peptide class IIb bacteriocins. *J. Med. Chem.* **2011**, *54*, 2399−2408.
(52) Kocbek, P.; Obermajer, N.; Cegnar, M.; Kos, J.; Kristl, J. Targeting cancer cells using PLGA nanoparticles surface modified with monoclonal antibody. *J. Controlled Release* **2007**, *120*, 18−26.